

# 2-hydroxyethylammonium oleate protic ionic liquid as corrosion inhibitor for aluminum in neutral medium

Maria R. Ortega Vega<sup>1</sup>  | Silvana Mattedi<sup>2</sup>  | Roberto M. Schroeder<sup>1,3</sup> | Célia de Fraga Malfatti<sup>1</sup> 

<sup>1</sup>Laboratório de Pesquisa em Corrosão (LAPEC), Department of Metallurgy, Universidade Federal do Rio Grande do Sul (UFRGS), Porto Alegre, Rio Grande do Sul, Brazil

<sup>2</sup>Laboratório de Termodinâmica Aplicada, Department of Chemical Engineering, Universidade Federal da Bahia (UFBA), Salvador, Bahia, Brazil

<sup>3</sup>Department of Mechanical Engineering, Pontifícia Universidade Católica do Rio Grande do Sul (PUCRS), Porto Alegre, Rio Grande do Sul, Brazil

## Correspondence

Maria R. Ortega Vega, Laboratório de Pesquisa em Corrosão (LAPEC), Department of Metallurgy, Universidade Federal do Rio Grande do Sul (UFRGS), Av. Bento Gonçalves 9500, Block 4, Bldg 43 427, Porto Alegre, RS, Brazil.  
Email: ortega.vega@ufrgs.br

## Funding information

Conselho Nacional de Desenvolvimento Científico e Tecnológico, Grant/Award Numbers: 306640/2016-3, 307723/2018-6; Coordenação de Aperfeiçoamento de Pessoal de Nível Superior, Grant/Award Numbers: 23038.000341/2019-71, 88887.463867/2019-00, PROEX0146048

## Abstract

Protic ionic liquid (PIL) 2-hydroxyethylammonium oleate (2HEAOI) proved to be a good lubricant for aluminum-forming processes. However, with the aim of keeping the formed component integrity, it is interesting that the same substance employed during forming does not need to be removed and works out as corrosion inhibitor. Then, the aim of this study was to test the performance of 2HEAOI as corrosion inhibitor for aluminum in neutral 0.5 mol/L NaCl medium by electrochemical characterization. Results showed that the concentration of  $5 \times 10^{-4}$  mol/L was a suitable concentration to promote corrosion inhibition until 72 h at the high chloride concentration studied. The PIL worked out as mixed-type organic corrosion inhibitor, as it promoted the diminution of the oxygen reduction reaction rate and, in consequence, the pit initiation by its adsorption on the metal surface.

## KEYWORDS

aluminum, corrosion inhibition, electrochemical impedance spectroscopy, pitting corrosion, protic ionic liquids (PILs)

## 1 | INTRODUCTION

Aluminum native oxide, mainly composed of  $\text{Al}_2\text{O}_3$  with a thickness between 5 and 100 Å,<sup>[1]</sup> works out as a protective film against environmental attack and maintains the structural integrity of the base metal when pH values are between 5 and 8.<sup>[2,3]</sup> However, when in presence of some kinds of aggressive species like halogen anions, the passive layer can be attacked

by localized corrosion in form of pits<sup>[4,5]</sup> that bring about problems in the normal operation of facilities and devices.

As most industries where aluminum is employed expose the metal to aggressive environments, it is important to carry out strategies to allow corrosion control, like the selection and use of corrosion inhibitors. Much has been studied about the use of corrosion inhibitors for aluminum-based materials with different organic substances<sup>[6–15]</sup> with good results, due

to interactions between the inhibitor molecules and the substrate.

Zheludkevich et al.<sup>[7]</sup> evaluated 1,2,4-triazole, 3-amino-1,2,4-triazole, benzotriazole and 2-mercaptobenzothiazole as corrosion inhibitors for AA2024 alloy in neutral chloride electrolyte; the inhibitors avoided dealloying of the copper-based intermetallics and retarded oxygen reduction reaction. 1,4-naphthoquinone<sup>[8]</sup> has been tested on aluminum and it worked out by shifting toward higher corrosion and pitting potential values compared to only sodium chloride electrolyte, as well as by reinforcing the passive layer. Other work<sup>[10]</sup> compared organic corrosion inhibitors, like salicylaldehyde, 8-hydroxyquinoline and quinaldic acid, to rare-earth nitrates, and the authors observed that organic substances reinforced passivation and prevention of intermetallics dissolution better than rare-earth nitrates. The addition of both 8-hydroxyquinoline and benzotriazole in aqueous electrolyte-enhanced passivation region inhibited oxygen reduction, and avoided intermetallic dissolution of AA2024, as reported by Marcelin and Pebère.<sup>[15]</sup>

Most of the mentioned organic corrosion inhibitors were reported to work out by adsorption, promoted by the presence of oxygen- and nitrogen-based functional groups. The development of metal-organic interaction is enhanced with the presence of heteroatoms in functional groups.<sup>[6–15]</sup> Following these lines, protic ionic liquids present themselves as promising corrosion inhibitors because of the variety of functional groups inside their molecules.

Protic ionic liquids (PILs) can be defined as compounds formed by organic ions in most of the cases, with the presence of a proton capable of hydrogen bonding. Due to the presence of organic structures in both anion and cation, PILs possess functional groups that make them suitable for promoting Coulombic and covalent interactions with metals. This property is desirable for applications like lubrication<sup>[16–20]</sup> and for corrosion inhibition.<sup>[12,21–23]</sup> One of the advantages of the use of PILs for these applications is their low vapor pressure, which ensures low emission of organic compounds to the atmosphere, as well as their thermochemical stability. In addition, they can constitute another alternative for substituting chromate-based corrosion inhibitors and their cost is lower than that of other ionic liquids.

The PIL matter of this study was already tested in other work<sup>[16]</sup> as a lubricant for aluminum, with an important reduction of wear and friction. In addition, it is an important concern that also the material integrity after forming be maintained during transport and storage, which points out the need for a corrosion inhibitor. Therefore, the aim of this study was to analyze the electrochemical performance of an oleate-based PIL, 2-hydroxyethylammonium oleate—2HEAOI, as a corrosion inhibitor in neutral chloride medium, thinking of a substance that can be employed both as a

lubricant in metal-forming processes and corrosion inhibitor for the formed component. Electrochemical characterization of diluted PIL in NaCl solution was conducted followed by morphological characterization. 2HEAOI was composed of the oleate anion, coming from oleic acid, and 2-hydroxyethylamine as cation precursor; in other work, it yielded the reduction of 98% of wear compared to dry, nonlubricated condition.<sup>[16]</sup> Other groups have tested similar fatty acid-based ionic liquids as lubricants: tetraalkylammonium oleates has been reported to be promising lubricants for steel tribopair,<sup>[24]</sup> stearic and palmitic acid-derived ionic liquids have been proved to reduce wear down to 80% when employed as additives in water,<sup>[18]</sup> and bis-2-hydroxyethylammonium oleate has been employed in graphene dispersions for steel contacts.<sup>[25]</sup> Other works also report the use of ethoxylated fatty acid as corrosion inhibitors for mild steel in sulfuric acid, with an efficiency of 96% at  $1 \times 10^{-3}$  mol/L of inhibitor.<sup>[26]</sup> Fatty acid triazoles were tested by other researchers as corrosion inhibitors for mild steel in hydrochloric and sulfuric acids with efficiency higher than 85%.<sup>[27]</sup> Citric and argaric acid were also studied as corrosion inhibitor for aluminum pigments, due to its capability of forming an aluminum chelate, to reduce hydrogen evolution in alkaline medium.<sup>[28]</sup>

In other work conducted by our group,<sup>[21]</sup> the performance of other oleate-based, ammonium-based PILs as corrosion inhibitor was tested for mild steel in contact with 0.01 mol/L NaCl. In that work, the tested PILs belong to the same oleate family (bis-2-hydroxyethylammonium oleate—BHEAOI and *N*-methyl-2-hydroxyethylammonium oleate—*m*-2HEAOI), but corrosion inhibition performance for steel differ to that for aluminum due to the different nature of the metals, as well as other experimental parameters. In consequence, this study also pointed out important similarities and differences between the corrosion mechanisms as well as the different inhibitor performance for both metals. PIL reported in this study, 2HEAOI, has not been tested before as corrosion inhibitor for aluminum in neutral medium and this application is subject of a deposited patent at the Brazilian intellectual property responsible entity (Instituto Nacional da Propriedade Intelectual [INPI]) number BR 10 2019 015605 8. This patent deposit relates to the use of carboxylate and amino-based protic ionic liquids, like those carboxylates coming from fatty acids, as corrosion inhibitors in aqueous media for metallic materials, which can be employed in different industrial applications (heat exchangers, water distribution, automotive, and mechanical sectors, etc.).

## 2 | EXPERIMENTAL

Oleate-based PIL 2-hydroxyethylammonium oleate (2HEAOI) was synthesized by Brønsted neutralization

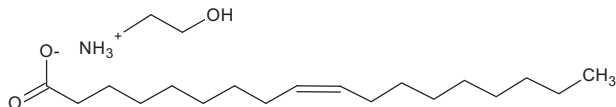


**FIGURE 1** Structure of protic ionic liquid 2HEAOI (2-hydroxyethylammonium oleate)

of an amine and a carboxylic acid, and its structure is shown in Figure 1. The structural characterization was confirmed by nuclear magnetic resonance and Fourier transform infrared (FTIR) spectroscopy; these results can be found elsewhere,<sup>[16]</sup> where it was tested as lubricant with a good result concerning low coefficient of friction and wear.

Aluminum 1100 samples with dimensions of  $30 \times 90 \times 1$  mm were used for the tests; alloy composition was already reported in other work.<sup>[29]</sup> Surface roughness of the samples was measured with a Bruker Contour GT-K optical interferometer and the image analysis was done with Vision64 software. Sz parameter was considered as the main factor to study as it corresponds to the peak–valley roughness.<sup>[30]</sup> Samples were used as received and they were washed with acetone, ethanol, and water, and dried with fresh air.

The electrolyte was composed of 0.5 mol/L sodium chloride solution with the addition of 2HEAOI in concentration of  $5 \times 10^{-5}$  or  $5 \times 10^{-4}$  mol/L. Measurements with concentration of  $5 \times 10^{-3}$  mol/L were intended to be conducted but at this PIL concentration there was the formation of a second phase; thus, the study with this concentration was discarded. A blank solution without PIL addition was also tested for comparison. A three-electrode cell was used for the electrochemical tests, with saturated calomel electrode (SCE) as reference electrode and a platinum wire as counter-electrode. The electrochemical measurements were conducted with a potentiostat/galvanostat Autolab PGSTAT302N by Metrohm, using software NOVA 1.11. All the electrochemical tests were carried out at least three times and only the data set with the most corroded aspect observed by microscopy was presented.

Open circuit potential (OCP) monitoring was conducted for 15 min. Then potentiodynamic polarization experiments were conducted between  $-400$  mV and  $+600$  mV versus OCP, with a scan rate of 1 mV/s.

Electrochemical impedance spectroscopy (EIS) was also measured with previous OCP measurement for until 20 min before each measurement. Sinusoidal perturbation of 7 mV (rms) from 100 kHz down to 10 mHz, with maximum time to reach a steady state of 30 s, was applied at OCP and 10 points per frequency decay were acquired.

Scanning electron microscopy (SEM) images of the aluminum samples after polarization tests were acquired employing a JEOL JSM5050. Optical interferometer was also employed to determine the pit depth.

### 3 | RESULTS AND DISCUSSION

#### 3.1 | Electrolyte characterization

The pH and conductivity of the electrolytes are listed in Table 1. In general, the presence of PIL at the highest concentration tested, yielded the increase of pH value in one unit. These PILs tend to be more alkaline because of the presence of the electron-donor amino group in the cation moiety. The studied pH values promoted the stability of the oxide film layer and, thus, made the pitting corrosion mechanism to predominate.<sup>[2,31]</sup> Conductivity remained almost the same with the PIL addition to the NaCl solution; it reveals that this PIL is not as good electrical ionic conductor as other ionic liquids, maybe due to the big size of the molecule.

#### 3.2 | OCP and potentiodynamic polarization measurement

Open circuit potential and polarization curves for the studied electrolytes appear in Figure 2. NaCl electrolyte promoted the biggest oscillation of OCP values during the first 5 min of immersion, which reduced with time until the sample reached an OCP value of  $\sim -725$  mV (Figure 2a). Similar corrosion potential in inhibitor-free chloride electrolyte was found for aluminum alloy 7075 in 0.05 mol/L NaCl by other authors.<sup>[32]</sup> The addition of the PIL at the lower concentration promoted even more oscillation than the noninhibited solution, maybe associated to the first contact of the solution with the aluminum passive layer and the short time considered for the measurements. During this first contact between the aluminum 1100 electrode and the electrolytes of only NaCl and NaCl with PIL at lower concentration, OCP instability could have been caused by the competing

**TABLE 1** pH and conductivity values of the studied electrolytes, with standard deviation in parenthesis

Inhibitor concentration (mol/L)	pH <sup>a</sup>	Conductivity (mS·cm) <sup>a</sup>
0	6.32 (0.10)	14.05 (4.00)
$5 \times 10^{-5}$	6.75 (0.33)	14.65 (5.12)
$5 \times 10^{-4}$	8.25 (0.4)	13.00 (4.17)

<sup>a</sup> $T = 22^\circ\text{C}$ .

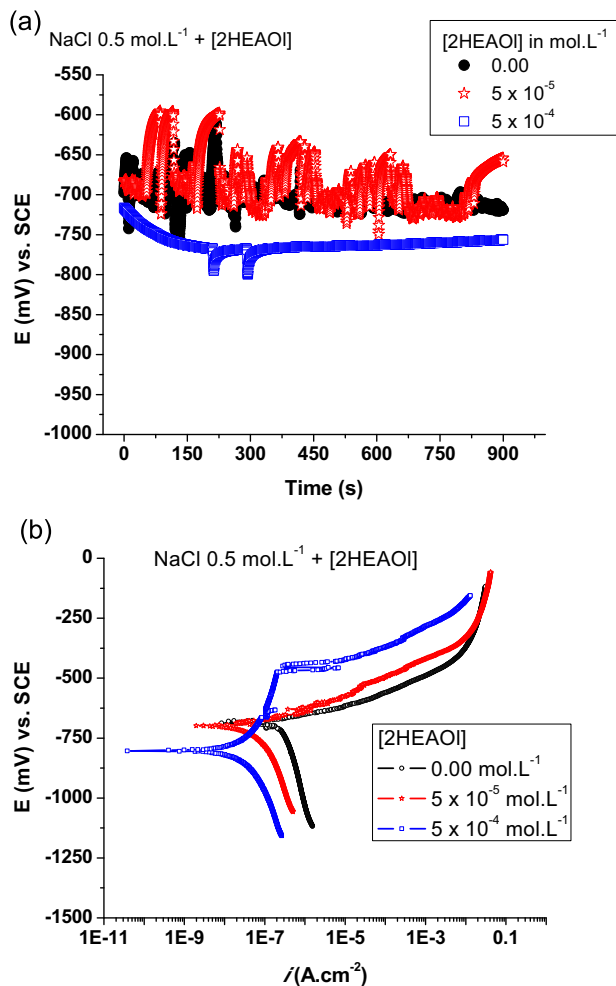


**FIGURE 2** (a) Open circuit potential and (b) polarization curve for the aluminum samples in contact with sodium chloride solution in absence and presence of different 2-hydroxyethylammonium oleate (2HEAOI) concentrations [Color figure can be viewed at [wileyonlinelibrary.com](http://wileyonlinelibrary.com)]

reactions of passive layer rupture by the chloride anions, with pit initiation, and the pit repassivation.<sup>[4,33,34]</sup> Because the same OCP variation was not observed for NaCl with 5 × 10<sup>-4</sup> mol/L 2HEAOI, which could be attributed to the formation of a uniform adsorbed layer of the organic compound that could hinder the formation of incipient pits and promote the stability observed in Figure 2a.

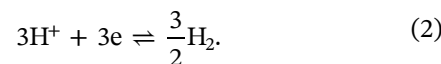
On the contrary, the addition of 5 × 10<sup>-4</sup> mol/L 2HEAOI (Figure 2a) shifted the potential toward more negative values during the first minutes of the experiment, possibly due to the modification of the structure of the passive layer,<sup>[35]</sup> or due to a more accentuated reduction of the kinetics of the cathodic processes, than of the anodic ones.<sup>[36]</sup> After 10 min, OCP values showed a slight increase. This increase can be attributed to the formation of an adsorbed layer of PIL on the hydrated passive layer or to a modification of the oxide

layer in the presence of an organic inhibitor, which compensates the more intense influence on the cathodic processes. OCP decrease with increasing PIL concentration could be related to the strong adsorption of the organic molecule on the Helmholtz plane.<sup>[37]</sup> The trend of lower corrosion potential was formerly reported by other researchers for inhibited sodium chloride electrolyte, employing hydroxyquinoline<sup>[38]</sup> versus the noninhibited condition.

Polarization curves are displayed in Figure 2b. Cathodic branches of the curves revealed that the oxygen reaction was inhibited in the presence of PIL as inhibitor (Figure 2b), as the limiting currents diminished when compared to the medium in absence of inhibitor, as observed in other works.<sup>[7]</sup> In addition, limiting currents decrease was more pronounced inasmuch as the inhibitor concentration increases, in agreement with the literature, for the employment of fatty acids as corrosion inhibitors for chloride medium (1 mol/L HCl).<sup>[39]</sup> This oxygen reduction inhibition is crucial for retarding pit formation.<sup>[31,40]</sup> Oxygen reduction is necessary for the formation of enough OH<sup>-</sup> species to favor the aluminum dissolution, as initially showed by Edeleanu and Evans,<sup>[39]</sup> later elucidated by other authors,<sup>[41,42]</sup> and expressed in the following equation:



and the counter-reaction is the hydrogen evolution, as exposed in the below equation,



Corrosion currents at corrosion potential were also reduced in the presence of PIL, with concentration being the main factor to reach more important corrosion current decreases down to one order of magnitude with 5 × 10<sup>-4</sup> mol/L 2HEAOI. Corrosion potential values were closer to those found during OCP monitoring. This behavior was also observed in other works.<sup>[37,39]</sup>

Anodic branch of the curve showed different profiles (Figure 2b). With the addition of 5 × 10<sup>-5</sup> mol/L the anodic behavior was similar to that observed in absence of inhibitor. For the curve with 5 × 10<sup>-4</sup> mol/L 2HEAOI, anodic branch developed a passive region, extended for overpotential of 329 mV, with passive currents in the order of 10<sup>-7</sup> A/cm<sup>2</sup>. Values of corrosion potential, pitting potential, and passive region overpotential are displayed in Table 3. *E*<sub>pit</sub> values found for 5 × 10<sup>-4</sup> mol/L 2HEAOI were closer to those reported in the literature.<sup>[6]</sup>

Then, at concentration of 5 × 10<sup>-4</sup> mol/L, PIL 2HEAOI allowed the separation of pitting potential. This phenomenon was not observed at lower inhibitor concentration or

**TABLE 2** Corrosion potential, pitting potential, and passive region overpotential values obtained from polarization curves

Inhibitor concentration (mol/L)	$E_{\text{Corr}}$ (mV) vs. SCE	$\Delta E_{\text{pass}}$ (mV) vs. SCE	$E_{\text{pit}}$ (mV) vs. SCE
0	-679	-	-
$5 \times 10^{-5}$	-698	-	-
$5 \times 10^{-4}$	-803	329	-474

in only NaCl medium in which pitting potential was lower than the corrosion potential, and the passive region was absent. Similar behavior was also reported by other authors.<sup>[43,44]</sup> The observed passive behavior can be attributed to the formation of an adsorbed, organic film on the aluminum surface. This layer suffered breakdown when potential reached pitting potential, value at which current increases in more than one order of magnitude with small potential variation.<sup>[45,46]</sup> The difference between pitting and corrosion potentials ( $\Delta E_{\text{pass}}$  in Table 2) is considered as an indicator for inhibitor efficiency against pitting corrosion, according to the literature.<sup>[38]</sup> When corrosion and pitting potential are convoluted at spontaneous conditions, pits will appear on the metal surface, as in the case of NaCl solution in absence of inhibitor; but the presence of the inhibitor promoted the shifting of the corrosion potential toward the cathodic direction. This separation allowed the protection of the substrate for the case of addition of  $5 \times 10^{-4}$  mol/L 2HEAOI to the electrolyte: at spontaneous conditions, no pit formation will be expected.<sup>[47]</sup>

With the addition of  $5 \times 10^{-4}$  mol/L 2HEAOI, pH increased one order of magnitude when compared to  $5 \times 10^{-5}$  mol/L and two orders when compared to the

**TABLE 3** Area covered by pits and average pit depth for aluminum 1100 samples after OCP monitoring and potentiodynamic polarization

Inhibitor concentration (mol/L)	Area covered by pits (%) <sup>a</sup>	Average pit depth ( $\mu\text{m}$ ) <sup>b</sup>	Sz ( $\mu\text{m}$ ) <sup>c</sup>
Clean aluminum			8.29 (0.72)
0	11	6.90 (2.04)	16.93 (2.42)
$5 \times 10^{-5}$	2.8	10.98 (4.45)	20.77 (2.98)
$5 \times 10^{-4}$	1.57	2.27 (0.35)	7.33 (1.18)

<sup>a</sup>Total area: 2.8 mm<sup>2</sup>. Determined by image analysis of the optical micrographs employing ImageJ.

<sup>b</sup>Determined by optical interferometry results. Standard deviation in parentheses.

<sup>c</sup>Peak-valley surface roughness, determined by optical interferometry. Sz for aluminum 1100 plate: 8.30  $\mu\text{m}$ .

NaCl solution, for which it could be expected that it would enhance passive behavior.<sup>[44]</sup> In fact, pH was a response of the system to the addition of 2HEAOI at the corresponding concentration. No pH adjustment was done because the new value did not affect the corrosion mechanism, expected to be pitting corrosion and confirmed by the electrochemical results. Some authors<sup>[48]</sup> relate that the pH increase promoted by the inhibitor addition did not modify the pitting potential and that only the presence of the inhibitor enhanced passivation. Similar results were found in other work of our group, employing other oleate-based PILs as corrosion inhibitor for mild steel.<sup>[21]</sup> In that work, inhibitor performance was independent of the pH increase caused by its addition and exclusively depended on the organic substance adsorption. According to some researchers,<sup>[1,49]</sup> isoelectric point for the aluminum passive layer is reached at pH 9.5; lower values promote that the oxide film possesses positive charge. In consequence, chloride ions as well as polar organic compounds can be adsorbed on the substrate surface during polarization,<sup>[43]</sup> which protects the substrate against the aggressive medium. Even though pH did not appear to enhance passivation, it can be favorable for PIL adsorption.

### 3.3 | Morphological characterization

Optical and SEM micrographs of the samples after potentiodynamic polarization in 0.5 mol/L NaCl are displayed in Figure 3. Optical microscopy showed (Figure 3a) important pits on the surface, observed as black spots on the metallic surface, some of them with diameter superior to 100  $\mu\text{m}$ . SEM images were employed to evaluate the pit morphology, as shown in Figure 3b,c). Pits were deep and presented important lateral growth (Figure 3b) perhaps due to coalescence; these phenomena can be a consequence of the autocatalytic nature of the pit.<sup>[45]</sup> In addition, pits presented in the form of inverted fir-tree and their growth is faceted (Figure 3c). Some authors reported this aspect of the pits developed on aluminum alloys surfaces when exposed to halide-containing electrolytes and attributed it to the preferential growth following determined crystal planes.<sup>[42,45,46,50]</sup>

Samples in contact with electrolyte in presence of inhibitor showed a cleaner surface, with less spots related to pitting corrosion, as observed on the optical micrographs of Figures 4a and 5a for concentrations  $5 \times 10^{-5}$  and  $5 \times 10^{-4}$  mol/L 2HEAOI, respectively. Image analysis software ImageJ was employed to determine the area covered by pits for the optical micrographs and the results appear in Table 3. These results confirm that the presence of 2HEAOI as inhibitor in the electrolyte allowed the reduction of the

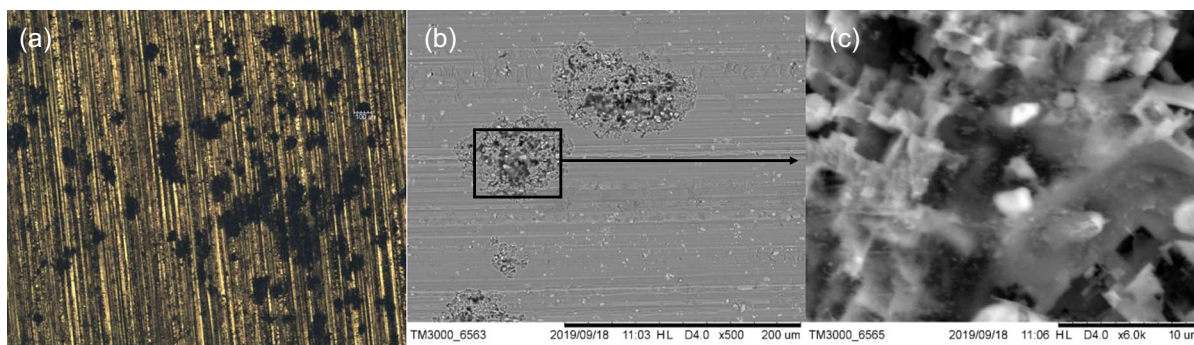


**FIGURE 3** (a) Optical microscopy and (b,c) scanning electron microscopy images of aluminum 1100 after potentiodynamic polarization measurements in 0.5 mol/L NaCl [Color figure can be viewed at [wileyonlinelibrary.com](http://wileyonlinelibrary.com)]

surface covered by pits, and higher the amount of 2HEAOI lesser was the pit formation on the substrate.

SEM micrograph of the sample after assay with solution containing  $5 \times 10^{-5}$  mol/L 2HEAOI (Figure 4b) showed a surface attacked by pits; however, these pits seem to have less lateral growth when compared to the surface after contact with NaCl electrolyte. The gross pits seem to be formed by the existence of lots of small pits. Even in the presence of the corrosion inhibitor, the formed pits presented preferential growth toward determined crystal planes (Figure 4c); this type of pit growth is typical of aluminum pits as reported by other authors.<sup>[42,45,46,50]</sup> In addition, the presence of the PIL allowed the formation of a white corrosion product at each pit boundary. In other work, the white corrosion product is associated with the formation of precipitates of NaCl with molecules of the organic compound.<sup>[51]</sup>

After electrochemical tests, aluminum samples in contact with inhibitor-free NaCl solution and with the addition of  $5 \times 10^{-5}$  mol/L 2HEAOI presented small particles on the surface that presented crystal-like shape (Figures 3b,c and 4b,c). Similar particles were also observed in the work of Baumgärtner and Kaesche,<sup>[52]</sup> developed at pitting potential

and at  $\pm 20$  mV versus pitting potential. Those authors reported that those small tunnels are constituted during the first stage of pit formation, caused by  $\text{Cl}^-$  adsorption on the aluminum surface. However, for pit growth it is necessary for it to achieve a volume and a surface; as some pits did not reach that critical size to grow, they appeared as small particles (Figures 3b,c and 4b,c). With the increase of potential, the density of tunnels increased, and the gross pit formation (Figures 3b and 4b) took place by coalescence of many tunnels that augmented the pit volume filled with acidic electrolyte.<sup>[41,52]</sup> In addition, these particles (Figures 3b,c and 4b,c) are not expected to be precipitates or second phases, given the absence of important amounts of alloy elements in the material composition.<sup>[29]</sup>

However, when in presence of the highest PIL concentration, the surface presented even less pit density (Figure 5a and Table 3) and the formed pits were the smallest-sized obtained when compared to those found with none and less inhibitor concentrations (Figures 3 and 4). Another factor that could have influenced the small pit sizes for concentration of  $5 \times 10^{-4}$  mol/L 2HEAOI as inhibitor was that pits had less time to grow in the studied conditions.<sup>[34]</sup>

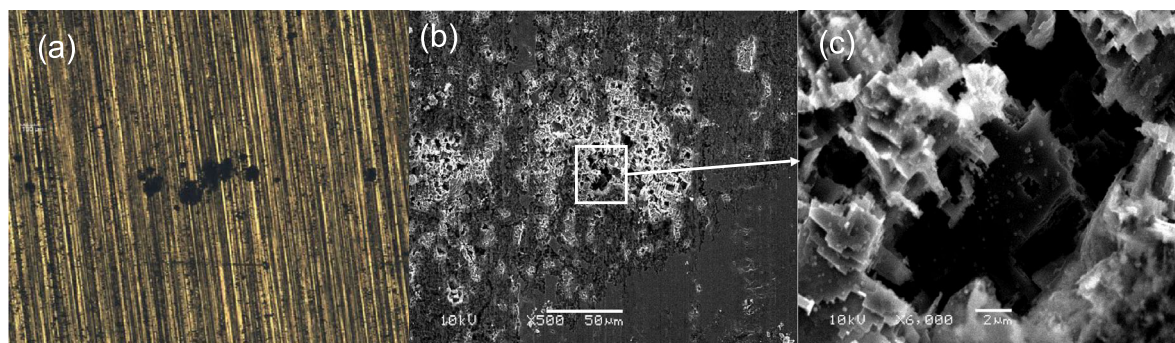
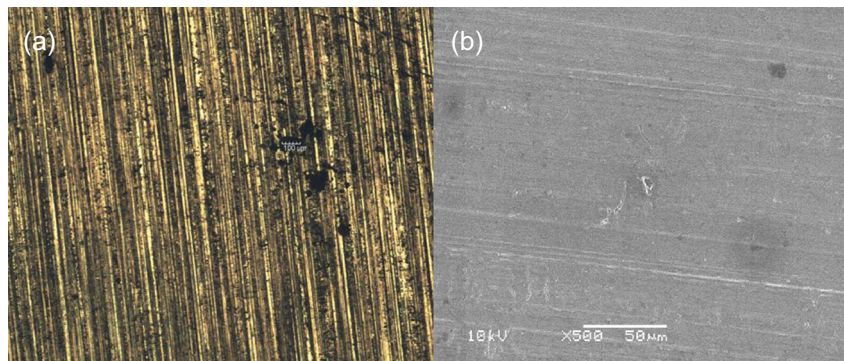


**FIGURE 4** (a) Optical microscopy and (b,c) scanning electron microscopy images of aluminum 1100 after potentiodynamic polarization measurements in 0.5 mol/L NaCl with addition of  $5 \times 10^{-5}$  mol/L 2HEAOI (2-hydroxyethylammonium oleate) as corrosion inhibitor [Color figure can be viewed at [wileyonlinelibrary.com](http://wileyonlinelibrary.com)]

**FIGURE 5** (a) Optical microscopy and (b,c) scanning electron microscopy images of aluminum 1100 after potentiodynamic polarization measurements in 0.5 mol/L NaCl with addition of  $5 \times 10^{-4}$  mol/L 2HEAOI (2-hydroxyethylammonium oleate) as corrosion inhibitor [Color figure can be viewed at [wileyonlinelibrary.com](http://wileyonlinelibrary.com)]



For this particular case, pits were nucleated at higher potentials (Figure 2b), almost at the end of the polarization experiment, without enough time to propagate.

Table 3 also shows the results obtained by optical interferometry. Average pit depth and variation of the peak–valley surface roughness<sup>[30]</sup> were appropriate indicators of the PIL performance as corrosion inhibitor. Pit depth was determined employing Vision64 software. It is noticeable that the presence of lower inhibitor concentration in the electrolyte promoted pits deeper than those obtained with only NaCl solution, which was not expected given the highest pit-covered area achieved with uninhibited medium. Other authors<sup>[45]</sup> reported that macroscopic pits can be formed even in presence of inhibiting agents and that tunneling toward the inside of the substrate was enhanced. In consequence, peak–valley surface roughness was increased with pit density (Table 4), given the important damage of the material, for the lower 2HEAOI concentration and for the only NaCl solution. On the contrary,  $5 \times 10^{-4}$  mol/L 2HEAOI appeared to be an efficient concentration to form a more uniform adsorbed layer that could overcome the pit nucleation and retard the pit growth; in consequence, less pit density was obtained and pit depth was the lowest at the studied conditions. In addition, the roughness compared to the aluminum plate before the electrochemical tests suggested that the presence of this concentration of PIL could keep the plate finishing (Table 4), in contrast to the other studied electrolytes for which the surface roughness was higher and presented important surface damage.

### 3.4 | Discussion considering the metal

When comparing the OCP results concerning the use of oleate-based PILs as corrosion inhibitors between steel<sup>[21]</sup> and aluminum, whereas the presence of PIL shifted potentials toward the anodic region for the former, the opposite effect was observed for the latter and OCP tended to remain lower than the bare alloy. Supporting information presents the results of OCP and polarization for the same aluminum alloy in 0.5 mol/L NaCl with the addition of PILs BHEAOI and m-2HEAOI (bis-2-hydroxyethylammonium oleate and methyl-2-hydroxyethylammonium oleate), studied for mild steel. In a former work, BHEAOI and m-2HEAOI were tested with 2HEAOI as lubricants for aluminum-forming processes.<sup>[16]</sup> Those PILs, as well as 2HEAOI subject of this study, yielded more negative values than, or even the same value of OCP for NaCl in absence of inhibitor when aluminum was the substrate, at concentrations of  $5 \times 10^{-4}$  and  $5 \times 10^{-5}$  mol/L, respectively. In the case of mild steel, for the same PIL concentration, OCP values were higher than that of the inhibitor-free medium.<sup>[21]</sup>

According to the literature<sup>[21,36,53–55]</sup> OCP shift is related to stability of the surface layers of the inhibitor and the oxide and to which reaction is favored, whether anodic or cathodic. Taking into account the results found in this study and in the literature,<sup>[53–57]</sup> this shift depends on the whole set of inhibitor molecule, metallic substrate, and electrolyte composition and properties. For example, in the case of mild steel, caffeic acid in 0.1 mol/L  $H_2SO_4$  promoted OCP shift toward negative values<sup>[54]</sup>; meanwhile, other works

**TABLE 4** Values for the components of the equivalent electrical circuit used to fit the electrochemical impedance spectra for sample immersed in NaCl 0.5 mol/L

Time (hr)	Rel ( $\Omega \cdot \text{cm}^2$ )	R1 ( $\text{k}\Omega \cdot \text{cm}^2$ )	$Q_{\text{CPE1}}$ ( $\mu\text{F} \cdot \text{cm}^{-2} \cdot \text{s}^n$ )	$n_{\text{CPE1}}$	R2 ( $\text{k}\Omega \cdot \text{cm}^2$ )	$Q_{\text{CPE2}}$ ( $\mu\text{F} \cdot \text{cm}^{-2} \cdot \text{s}^n$ )	$n_{\text{CPE2}}$	$\chi^2 (\times 10^3)$
48	10.98	18.13	14.79	0.99	65.01	258	0.71	1.28
72	10.13	23.81	14.61	0.99	55.78	276	0.70	0.716
96	10.39	25.12	14.55	0.99	110.09	317	0.69	0.410

**TABLE 5** Values for the components of the equivalent electrical circuit fitted to the electrochemical impedance spectra for simple immersed in NaCl 0.5 mol/L + 2HEAOI  $5 \times 10^{-5}$  mol/L

Time (hr)	Rel ( $\Omega \cdot \text{cm}^2$ )	R1 ( $\text{k}\Omega \cdot \text{cm}^2$ )	$Q_{\text{CPE1}}$ ( $\mu\text{F} \cdot \text{cm}^{-2} \cdot \text{s}^n$ )	$n_{\text{CPE1}}$	R2 ( $\text{k}\Omega \cdot \text{cm}^2$ )	$Q_{\text{CPE2}}$ ( $\mu\text{F} \cdot \text{cm}^{-2} \cdot \text{s}^n$ )	$n_{\text{CPE2}}$	$Q_{\text{CPE3}}$ ( $\mu\text{F} \cdot \text{cm}^{-2} \cdot \text{s}^n$ )	$n_{\text{CPE3}}$	$\chi^2 (\times 10^3)$
48	9.57	29.18	25.93	0.86	1.44	8.99	0.80	312	0.49	0.722
72	9.40	22.38	27.30	0.90	1.61	10.1	0.77	417	0.46	0.430
96	7.27	20.28	29.73	0.91	1.61	11.5	0.75	455	0.43	0.335

employing 4-amino-5-phenyl-4H-1,2,4-triazole-3-thiol as corrosion inhibitor in 2.5 mol/L  $\text{H}_2\text{SO}_4$ , OCP was shifted for more positive potentials.<sup>[53]</sup> OCP increase can be expected by the absence of passive films on mild steel surfaces exposed to the atmosphere or to neutral aqueous medium<sup>[36]</sup>; thus, it is expected that the inhibitor action will be predominant on the anodic reactions and on generalized corrosion. On the contrary, aluminum naturally possesses a layer of protective passive oxide; hence, it can be expected that organic inhibitors that work out by adsorption more interfere in the cathodic processes than in the anodic ones, and in pits.<sup>[34]</sup>

For both aluminum and steel, OCP values and corrosion potentials determined by potentiodynamic polarization were close for each corresponding condition. Potentiodynamic polarization in both cases revealed the formation of a PIL layer that not only shifted corrosion potentials but promoted the corrosion current density decrease. In the case of steel, this corrosion current diminution is desirable, given that it represents the diminution of generalized corrosion, mechanism proper of steel. But in the case of aluminum, corrosion current was not significant when compared to pitting corrosion current.<sup>[58]</sup> For aluminum, corrosion current densities fell in the order of passive currents (Figure 2b, S1b and S2b),  $i_{\text{corr}} < 1 \times 10^{-6}$  A/cm<sup>2</sup> at inhibitor-free 0.5 mol/L NaCl solution; meanwhile, for steel in 0.01 mol/L NaCl, those values were higher than  $1 \times 10^{-6}$  A/cm<sup>2</sup>. For aluminum, corrosion current densities similar to the values found for steel were observed at the pitting potential, where the current density is proportional to the number of pits per unit area, as explained by Kaesche.<sup>[41]</sup> In consequence, all the approach considering corrosion current, that is, corrosion inhibition efficiency and adsorption isotherm calculations, was not considered the most adequate by the authors to include in the aluminum study.

Cathodic branches of the currents for aluminum displayed important oxygen reduction inhibition (Figure 2b, S1b, and S2b), reaction that is involved in the substrate dissolution process. It means that the inhibition of oxygen reduction is related to the delay of pit formation and propagation,<sup>[31]</sup> which was found to be the mechanism followed in presence of all the oleate-based PILs. When steel

was the studied substrate, oxygen reduction was not affected by the presence of inhibitor as strongly as it was in the case of aluminum, even in higher concentration of inhibitor ( $5 \times 10^{-3}$  mol/L), as smaller reductions of limiting current of this reaction were observed.<sup>[21]</sup>

Anodic branches, however, followed similar trends for both aluminum (Figure 2b, S1b, and S2b) and steel.<sup>[21]</sup> Both polarization curves displayed the presence of an adsorbed layer of PIL that broke at the pitting potential, where current density was increased even with small increases in potential (10 mV, for example). In both cases, the passive region was extended with an increase in PIL concentration. In case of steel, PIL concentration also influenced the fraction of the surface covered by the PIL or surface coverage parameter ( $\theta$ ). An analogous approach could be employed for the case of the aluminum, where, at the studied conditions, the extension of the passivation region can be related to the surface coverage, but more studies need to be conducted to prove this hypothesis and find a possible correlation. Then, BHEAOI could have yielded better coverage than m-2HEAOI, given the passivation region of 271 and 220 mV at concentration of  $5 \times 10^{-4}$  mol/L, as shown in Table S1; but it still could not surpass the performance of 2HEAOI, with 329 mV as passive region at the same concentration (Table 2).

Morphology characterization of both metals after potentiodynamic polarization tests reinforce the importance of the electrolyte composition, pH, and inhibitor concentration. For steel in only 0.01 mol/L NaCl, general corrosion was observed; when in presence of PILs, surfaces had a smoother aspect and lower roughness than the as-prepared sample but surfaces developed localized corrosion.<sup>[21]</sup> For the case of aluminum in the presence of only 0.5 mol/L NaCl, the surface was 11% covered with pits. With PIL addition at the higher concentration, area covered by pits could not be determined and pit depth was hard to separate from roughness, similar to the results found for steel. But at the low concentration studied, no important inhibition effect was observed and pits deeper than those found in NaCl were seen (Tables 2 and S2). This low concentration was not even studied for steel and only important inhibition effect was seen at  $5 \times 10^{-4}$  mol/L in both metals.



**TABLE 6** Values for the components of the equivalent electrical circuit fitted to the electrochemical impedance spectra for simple immersed in NaCl 0.5 mol/L + 2HEAOl +  $5 \times 10^{-4}$  mol/L

Time (hr)	Rel ( $\Omega\text{-cm}^2$ )	R1 ( $k\Omega\text{-cm}^2$ )	Q <sub>CPE1</sub> ( $\mu\text{F}\cdot\text{cm}^{-2}\cdot\text{s}^n$ )	n <sub>CPE1</sub>	R2 ( $k\Omega\text{-cm}^2$ )	Q <sub>CPE2</sub> ( $\mu\text{F}\cdot\text{cm}^{-2}\cdot\text{s}^n$ )	n <sub>CPE2</sub>	R3 ( $k\Omega\text{-cm}^2$ )	Q <sub>CPE3</sub> ( $\mu\text{F}\cdot\text{cm}^{-2}\cdot\text{s}^n$ )	n <sub>CPE3</sub>	$\chi^2$ ( $\times 10^3$ )
48	7.10	-	-	-	0.564	8.825	0.72	7681.06	4.22	0.94	2.27
72	6.46	0.221	3.205	0.83	1.24	19.7	0.71	1071	7.14	0.90	0.955
96	6.75	0.173	1.827	0.86	0.914	13.6	0.72	54.06	11.34	0.79	0.860

On the contrary, even after longer tests for the aluminum, it was not observed a layer as thick as in the case of steel, as it could not be by spectroscopy techniques (Raman and FTIR). In consequence, structural characterization to determine the composition of the corrosion products was not possible.

### 3.5 | EIS

Initially, OCP presented lower values than when in presence of uninhibited medium and it tended to increase until the end of the experiment (Figure 6); this potential increase can be attributed to the formation of corrosion product to the point of reaching the same OCP of the 0.5 mol/L NaCl (216 hr). Other authors<sup>[15]</sup> reported similar behavior for AA2024T3 alloy in inhibited 0.1 mol/L Na<sub>2</sub>SO<sub>4</sub> + 0.05 mol/L NaCl solution, employing hydroxyquinoline and benzotriazole as corrosion inhibitors, and even in exclusive presence of organic compounds in water as in the case of sodium oxalate.<sup>[36]</sup> Stable EIS response was obtained since 48 hr of immersion; for this reason, results will be showed starting at this time, and recorded until the appearing of pitting at higher PIL concentration (96 hr); however, OCP was monitored until 264 hr, when potentials for all the studied cases yielded to be close to one another, aiming to confirm that the protection did not work anymore.

Impedance spectra for NaCl (Figure 7) were similar to those presented by other researchers at 20<sup>[15]</sup> and by 48 hr.<sup>[7]</sup> The spectra were characterized along the whole experiment by one capacitive arc in high and medium frequencies, related with the formation of corrosion product on the metal surface, and by a diffusion-related phenomenon at low frequency. No inductive arc at low frequency was displayed in the shown spectra of Figure 7. This characteristic was also reported in other works, due to the ceasing of hydrogen bubbling on the cathodic sites around the pit regions that would be expected until the first 46 hr of immersion.<sup>[59]</sup>

Two semicircles were observed in presence of 2HEAOl in  $5 \times 10^{-5}$  mol/L (Figure 8), one of them attributed to the oxide film and the other one to pitting. In addition, at low frequency, diffusion was identified, as in the case of the medium without inhibitor.

With higher concentration ( $5 \times 10^{-4}$  mol/L; Figure 9), there was the formation of an important layer of PIL on the metal surface with insulating character that promoted the development of an uncompleted semicircle at 48 hr. However, the size of this arc reduced with time and lasted until 72 hr. At 96 hr, the impedance arc presented the same profile as those arcs for the lower concentration; thus, pitting corrosion took place and allowed the important reduction of total resistance in, at least, one order

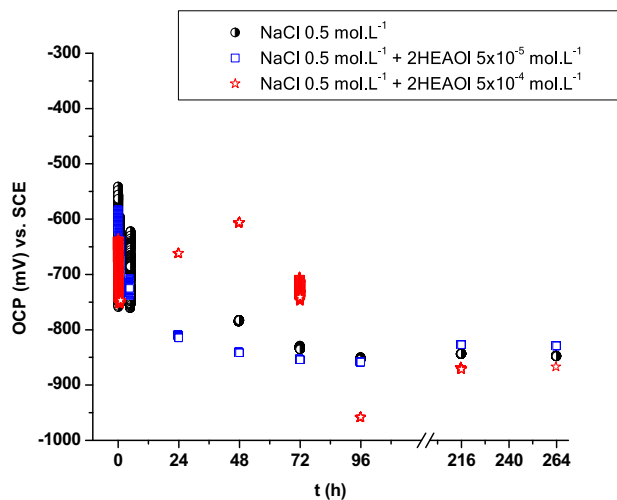


**FIGURE 6** Open circuit potential monitoring before electrochemical impedance spectroscopy analysis [Color figure can be viewed at [wileyonlinelibrary.com](http://wileyonlinelibrary.com)]

of magnitude. At 48 hr of immersion, sample with the highest amount of PIL as corrosion inhibitor had similar behavior as for the best inhibition performance of other compounds like triazole in 0.005 mol/L sodium chloride medium.<sup>[7]</sup> Better inhibition performance was found in this study than in the work of Zuo et al.,<sup>[48]</sup> where the authors tested sodium oleate as corrosion inhibitor in 0.1 mol/L NaCl and reported that for 48 h EIS spectrum of the inhibited sample was similar to that immersed in the only-chloride medium.

For better understanding of the phenomena that take place on the aluminum surface, fitting to equivalent electrical circuit was conducted employing ZView® software. The circuits employed to fit data appear in Figure 10 and the values for their components in Tables 4–6. The  $\chi^2$  parameter lower than  $1 \times 10^{-3}$  was the criterion for choosing the equivalent circuit. At high frequencies all the spectra showed an uncompensated resistance  $R_{el}$  attributed to the electrolyte resistance; PIL addition to the electrolyte brought about the slight decrease of  $R_{el}$ , attributable to its intrinsic conductivity, given the labile proton within.<sup>[60]</sup> Two time constants were observed for the system without inhibitor (Figure 10a), and when 2HEAOI is present, three phenomena appeared (Figure 10b,c). These results matched with the ones reported in the literature.<sup>[7,38,61]</sup> For modeling the time constants, constant phase elements (CPE) were employed instead of pure capacitors to consider surface irregularities; the impedance of CPEs is described by the following equation:

$$Z_{CPE} = \frac{1}{Q_{CPE}(\omega j)^n}, \quad (1')$$

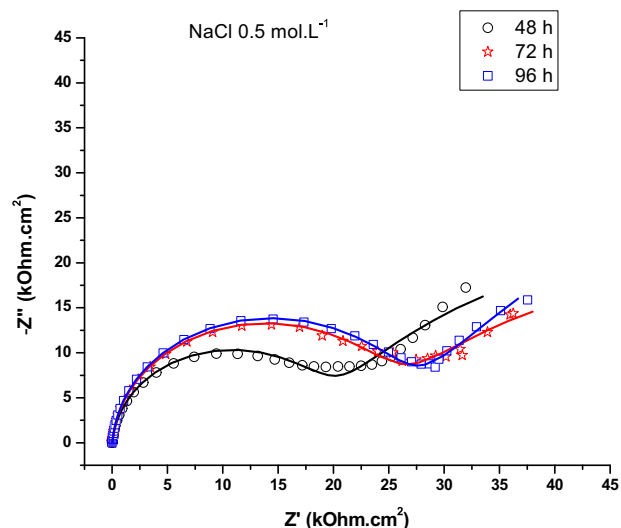


**FIGURE 7** Electrochemical impedance spectra for AA1100 in 0.5 mol/L NaCl after 48, 72, and 96 hr of immersion (fit results in solid lines) [Color figure can be viewed at [wileyonlinelibrary.com](http://wileyonlinelibrary.com)]

where  $Q_{CPE}$  corresponds to CPE admittance,  $n$  is the exponent related to the phase shift,  $\omega$  is the angular frequency and  $j = \sqrt{-1}$ .

For the chloride medium without inhibitor (Table 4) the first time constant (high frequency,  $R_1$ ,  $CPE_1$ ) can be associated to the passive layer on the aluminum substrate surface. Values found for the circuit elements associated with this time constant were similar to those presented by the literature and behaved stable after 46 hr.<sup>[7]</sup> Values for  $n_{CPE1}$

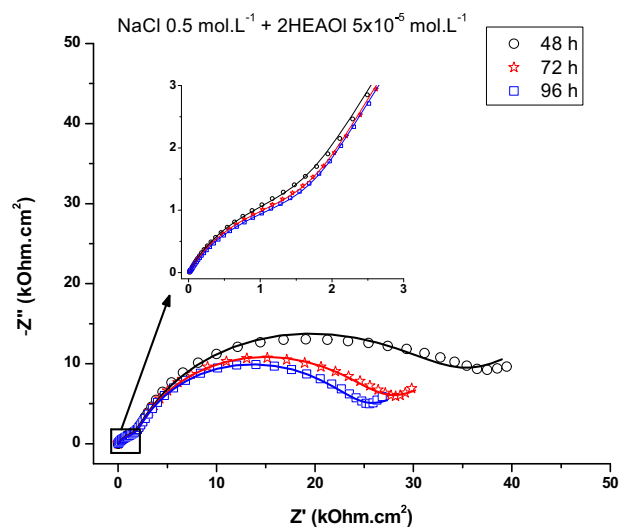


**FIGURE 8** Electrochemical impedance spectra for AA1100 in 0.5 mol/L NaCl + 2HEAOI  $5 \times 10^{-5}$  mol/L after 48, 72, and 96 hr of immersion (fit results in solid lines) [Color figure can be viewed at [wileyonlinelibrary.com](http://wileyonlinelibrary.com)]

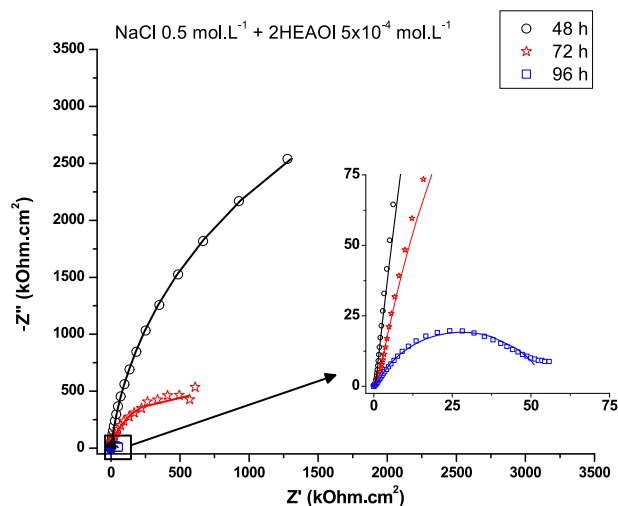


**FIGURE 9** Electrochemical impedance spectra for AA1100 in 0.5 mol/L NaCl + 2HEAOI  $5 \times 10^{-4}$  mol/L after 48, 72, and 96 hr of immersion (fit results in solid lines) [Color figure can be viewed at [wileyonlinelibrary.com](http://wileyonlinelibrary.com)]

allowed thinking about a uniform, dense oxide layer, due to the alloy type of the studied material, where no precipitates or second phases are expected that can form galvanic couples and enhance pitting formation like in the cases of Al-Zn-Mg,<sup>[61,62]</sup> Al-Mg-Si,<sup>[44]</sup> and Al-Cu<sup>[63–65]</sup> alloys. The second time constant presented characteristic diffusion-related  $n_{\text{CPE2}}$  values, getting close to 0.5. It can be associated with diffusion involving pits. According to Baumgärtner and Kaesche,<sup>[52]</sup> the inner part of the pit is rich in hydrated  $\text{AlCl}_3$  as a result of the solubility of the passive oxide  $\text{Al}_2\text{O}_3$  and of the aluminum dissolved during the pit formation; thus, a diffusion layer is formed at the pit entrance due to the different composition of the electrolyte inside and outside the pit. After 48 hr, no particular semicircle for pits was observed, as at this time, all the surface is expected to be covered by pits and the electrical

response is the total of the contributions of all pits on the surface area.<sup>[41]</sup>

Spectra for inhibited systems presented different arc profiles as well as circuits for fitting. When in presence of  $1 \times 10^{-5}$  mol/L 2HEAOI the circuit that best fitted the EIS results was that of Figure 10(b) and the values of its parameters appear in Table 5. Two time constants were observed. The first one, with similar values to that of the NaCl solution, probably related to the oxide layer modified by the electrolyte and the adsorbed PIL, given the higher  $R_1$  and  $Q_{\text{CPE1}}$  values. Lower values of  $n_{\text{CPE1}}$  compared to NaCl solution can be related to less homogeneous oxide layer when in presence of the organic substance, as reported in other works.<sup>[7,15]</sup> The second time constant, formed by the subcircuit (R2(CPE2)CPE3) can be associated with pitting corrosion and diffusion of the species from the inside of the pit toward the bulk of the electrolyte<sup>[41,52]</sup> that took place in one step.<sup>[66]</sup> The low R2 value is attributed to pitting where faradaic processes are concentrated and once started, they cannot be stopped given the autocatalytic nature of the pits.<sup>[34,40]</sup> The clear separation of this phenomenon, different to what occurred with only NaCl electrolyte, was attributed to the reduction of the area covered by pits, as well as to the deeper pits formed in presence of  $5 \times 10^{-5}$  mol/L 2HEAOI when compared to the inhibitor-free solution (Figure 4 and Table 3).

With higher 2HEAOI concentration,  $5 \times 10^{-4}$  mol/L, circuits with two (Figure 10a), for 48 hr, and three, for 72 and 96 hr, time constants (Figure 10c) gave away the best-fitting and the parameters for this equivalent circuit are listed in Table 6. At 48 hr, the circuit presented two time constants, probably associated to the oxide layer modified by the presence of the organic substance in the electrolyte (named as R3 and CPE3) that promoted the formation of an insulating film, seen as the uncompleted semicircle in Figure 9, which protected the surface from the solution attack. The oxide covered by the PIL retarded oxygen reduction, which promoted the high R3 value; these values are in agreement with those reported by other authors.<sup>[15]</sup> A component probably attributed to chloride diffusion on the oxide<sup>[36]</sup> was observed in the time constant formed by R2 and CPE2, as suggested by the  $n$  parameter, close to 0.5. Chloride diffusion is necessary for pitting initiation.<sup>[31,41,42]</sup>

At 72 hrs, insulating properties decreased as seen by the R3 and CPE3 values and pits started appearing as a new time constant (R1 and CPE1; Table 6). In the subcircuits associated with the pit for the inhibited medium  $n$  values were higher than 0.70, which can be possibly caused by the crystalline growth of the pit. Once again and as in the case of the lower concentration of the inhibitor, the pit component appeared independent of the other phenomena, given

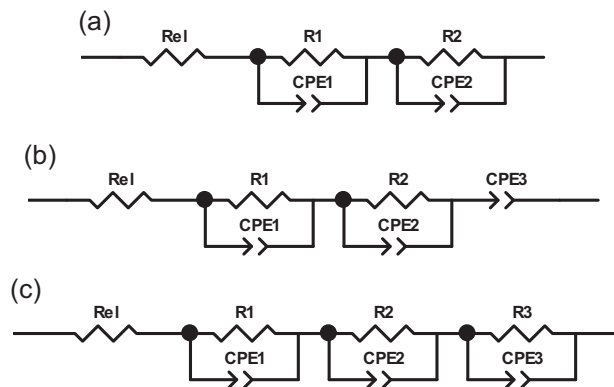


**FIGURE 10** Equivalent electrical circuits employed to fit electrochemical impedance spectroscopy data for all the studied systems

the lower number of pits per surface area observed in the inhibited system (Table 3 and Figure 5). The start of pitting at this time was preceded by the time constant formed by R2 and CPE2 at 48 hr. At 72 hr, circuit formed by R2 and CPE2 can be related to diffusion of species between the pit and the medium. Given that pitting appeared only after 72 hr, the presence of 2HEAOI seemed to retard the chloride arrival toward the surface and its diffusion through the oxide layer until this time. However, the studied chloride concentration is indicative of severe conditions that probably would not be expected in a practical scenario for aluminum 1100, which points out that the protection could last longer. In addition, R3 still presented a high value (1,071 k $\Omega$ /cm<sup>2</sup>); it means that at this time of immersion, oxygen reduction reaction was still strongly inhibited by the presence of inhibitor, with values in the order of those reported formerly in the literature.<sup>[15]</sup> As formerly reported by our group in other work, this inhibition could be promoted by the formation of a complex between the chloride anion and the PIL.<sup>[21]</sup>

At 96 hr of immersion in 0.5 mol/L NaCl +  $5 \times 10^{-4}$  mol/L 2HEAOI, fall of R3 and  $n_{\text{CPE3}}$  values (Table 6) for the component concerning the oxide layer with PIL adsorption (R3 and CPE3) showed that the layer lost its protective character. Subcircuits related to pits and diffusion kept stable until the end of the experiments, given the autocatalytic nature of the pit<sup>[34,40]</sup> and the diffusion of species between the pit inner part and the electrolyte.<sup>[41,52]</sup>

### 3.6 | Inhibition mechanism

Given all the former results, 2HEAOI worked out as corrosion inhibitor for aluminum in high chloride concentration until 72 hr, at a concentration of  $5 \times 10^{-4}$  mol/L. 2HEAOI can be considered as a mixed-type organic corrosion inhibitor, with predominance of cathodic inhibition (Figure 6), as its addition to the electrolyte promoted modifications on the rate of the cathodic reaction and, in consequence, modified the anodic mechanism.<sup>[36]</sup>

In the anodic mechanism, the important extension of the passive region (Figure 2), as well as the time necessary to chloride anions overcome the diffusion resistance (Figure 9 and Table 6) allow to state that the adsorbed layer of PIL at the highest concentration had an important coverage that could block the arrival of the chloride anions to the passive metal oxide layer. This phenomenon could take place by the reaction between the PIL and the chloride anions, as reported in other works.<sup>[21,67]</sup> The cation moiety of the PIL could be electrostatically attracted toward the chloride anions, through the amino functional group,<sup>[21,68]</sup> which retarded their arrival toward the surface. On the contrary, the counterion corresponding to the

oleate anion could have been chemisorbed on the substrate surface, given that, at the studied pH, aluminum possesses an excess of positive charge.<sup>[2,31]</sup> Considering pits, where acidification took place due to the anodic dissolution of aluminum and the formation of Al<sup>3+</sup>, the presence of chloride and the excess of H<sup>+</sup>, there could be the occlusion of the formed pit by the electrostatic attraction formed between the chloride ion and the amino function of the PIL, as reported for aluminum in acidic media by other authors.<sup>[68,69]</sup> It could explain the lower depth of pits obtained with the highest 2HEAOI concentration: after pit formation, 2HEAOI reacted with chloride anions and the product of the reaction could have occluded the pit and retarded the pit growth.

The results obtained in this study revealed that 2HEAOI can be an interesting corrosion inhibitor for aluminum in neutral even at high chloride concentration, a severe condition, as well as other similar oleate-based PILs were tested for steel.<sup>[21]</sup> This PIL allowed corrosion protection at high chloride concentration until 72 hr. This performance can be promising, considering that this PIL was initially thought of as lubricant for metal-forming processes<sup>[16]</sup> but it could also maintain the formed component material integrity working out as corrosion inhibitor.

## 4 | CONCLUSION

The studied PIL, 2HEAOI, successfully inhibited pitting corrosion on an aluminum substrate, when in contact with 0.5 mol/L NaCl electrolyte. 2HEAOI worked out as a mixed-type organic corrosion inhibitor. Its adsorption promoted the inhibition of the cathodic reaction, mainly the oxygen reduction, which is vital for pit formation. As a consequence, there was the enhancement of the passivation region at all the tested concentrations, which was attributed to the formation of a PIL adsorbed layer that blocked the chloride anions access to the substrate surface. When this blockage was overcome by the diffusion of the chloride ions through the adsorbed layer, pit started, which took place at pitting potential. EIS allowed the confirmation of the PIL layer formation and revealed that 72 hr were necessary for the chloride ions to initiate pitting at the highest PIL concentration ( $5 \times 10^{-4}$  mol/L). The surface that was in contact with inhibitor-free electrolyte presented the higher surface covered by pits (11%); this response was minimized with the increase of 2HEAOI concentration in the solution (undetermined for  $5 \times 10^{-4}$  mol/L 2HEAOI). The presence of PIL did not affect the pit morphology, as, for all the studied cases, crystalline pits, with inverted fir-tree shape were observed. A different mechanism of inhibitory action was found for aluminum when compared to steel. The presence of chloride in the electrolyte and of amino and carboxylic

functions were highly important for the PIL performance as a corrosion inhibitor.

## ACKNOWLEDGMENTS

The authors gratefully appreciate the support of Universidade Federal do Rio Grande do Sul (UFRGS) and Universidade Federal da Bahia (UFBA), as well as CAPES and CNPq for financial support. S. Mattedi acknowledges CNPq (Grant 306640/2016-3), C. F. Malfatti acknowledges CNPq (Grant 307723/2018-6), and Dr. Ortega Vega thanks for the doctorate scholarship CAPES PROEX0146048 and Postdoctorate scholarship CAPES PNPd (Grant 88887.463867/2019-00).

## ORCID

Maria R. Ortega Vega  <http://orcid.org/0000-0002-6049-2831>

Silvana Mattedi  <https://orcid.org/0000-0003-4816-7494>

Célia de Fraga Malfatti  <https://orcid.org/0000-0002-0819-479X>

## REFERENCES

- [1] E. McCafferty, P. M. Natishan, *ECS Trans.* **2011**, 33, 47.
- [2] M. Pourbaix, *Atlas of Electrochemical Equilibria in Aqueous Solutions*, Pergamon Press, New York, NY **1966**.
- [3] K. Xhanari, M. Finšgar, *RSC Adv.* **2016**, 6, 62833.
- [4] S. B. de Wexler, J. R. Galvele, *J. Electrochem. Soc.* **1974**, 121, 1271.
- [5] M. A. Streicher, *J. Electrochem. Soc.* **1956**, 103, 375.
- [6] A. A. El-Shafei, S. A. Abd El-Maksoud, A. S. Fouda, *Corros. Sci.* **2004**, 46, 579.
- [7] M. L. Zheludkevich, K. A. Yasakau, S. K. Poznyak, M. G. S. Ferreira, *Corros. Sci.* **2005**, 47, 3368.
- [8] E. M. Sherif, S. M. Park, *Electrochim. Acta* **2006**, 51, 1313.
- [9] L. Vrsalović, M. Kliškić, J. Radošević, S. J. Gudić, *Appl. Electrochem.* **2007**, 37, 325.
- [10] S. V. Lamaka, M. L. Zheludkevich, K. A. Yasakau, M. F. Montemor, M. G. S. Ferreira, *Electrochim. Acta* **2007**, 52, 7231.
- [11] S. Zor, H. Özkazanç, *Prot. Met. Phys. Chem. Surf.* **2010**, 46, 727.
- [12] Q. Zhang, Y. Hua, *Mater. Chem. Phys.* **2010**, 119, 57.
- [13] T. G. Harvey, S. G. Hardin, A. E. Hughes, T. H. Muster, P. A. White, T. A. Markley, P. A. Corrigan, J. Mardel, S. J. Garcia, J. Mol, A. M. Glenn, *Corros. Sci.* **2011**, 53, 2184.
- [14] I. Jevremović, V. Misković-Stanković, *Metall. Mater. Eng.* **2012**, 18, 241.
- [15] S. Marcelin, N. Pébère, *Corros. Sci.* **2015**, 101, 66.
- [16] M. R. Ortega Vega, J. Ercolani, S. Mattedi, C. Aguzzoli, C. A. Ferreira, A. S. Rocha, C. F. Malfatti, *Ind. Eng. Chem. Res.* **2018**, 57, 12386.
- [17] T. Espinosa, M. Jiménez, J. Sanes, A. E. Jiménez, M. Iglesias, M. D. Bermúdez, *Tribol. Lett.* **2014**, 53, 1.
- [18] M. D. Avilés, F. J. Carrión, J. Sanes, M. D. Bermúdez, *Wear* **2018**, 408–409, 56.
- [19] A. Khan, R. Gusain, M. Sahai, O. P. Khatri, *J. Mol. Liq.* **2019**, 293, 111444.
- [20] M. D. Avilés, F. J. Carrión-Vilches, J. Sanes, M. D. Bermúdez, *Tribol. Lett.* **2019**, 67, 26.
- [21] T. E. Schmitzhaus, M. R. O. Vega, R. Schroeder, I. L. Muller, S. Mattedi, C. F. Malfatti, *Mater. Corros.* **2020**, 1.
- [22] N. V. Likhanova, P. Arellanes-Lozada, O. Olivares-Xometl, H. Hernández-Cocolezzi, I. V. Lijanová, J. Arriola-Morales, J. E. Castellanos-Aguila, *J. Mol. Liq.* **2019**, 279, 267.
- [23] M. Nishita, S. Y. Park, T. Nishio, K. Kamizaki, Z. Wang, K. Tamada, T. Takumi, R. Hashimoto, H. Otani, G. J. Pazour, V. W. Hsu, Y. Minami, *Sci. Rep.* **2017**, 7, 1.
- [24] R. Gusain, O. P. Khatri, *RSC Adv.* **2016**, 6, 3462.
- [25] M. D. Avilés, A. E. Jiménez, N. Saurin, F. J. Carrión, J. Sanes, M. D. Bermúdez, *Tribol. Int.* **2018**, 105516.
- [26] E. E. Foad El Sherbini, *Mater. Chem. Phys.* **1999**, 60, 286.
- [27] M. A. Quraishi, D. Jamal, *J. Appl. Electrochem.* **2002**, 32, 425.
- [28] B. Müller, *Corros. Sci.* **2004**, 46, 159.
- [29] M. R. Ortega Vega, K. Parise, L. B. Ramos, U. Boff, S. Mattedi, L. Schaeffer, C. F. Malfatti, *Mater. Res.* **2017**, 20, 675.
- [30] Bruker Corporation, *Help*, Vision 64 5.60. **2014**.
- [31] M. C. Reboul, B. Baroux, *Mater. Corros.* **2011**, 62, 215.
- [32] O. Olivares-Xometl, C. López-Aguilar, P. Herrastí-González, N. V. Likhanova, I. Lijanová, R. Martínez-Palou, J. A. Rivera-Márquez, *Ind. Eng. Chem. Res.* **2014**, 53, 9534.
- [33] I. A. Maier, J. R. Galvele, *J. Electrochem. Soc.* **1978**, 125, 1594.
- [34] G. S. Frankel, *J. Electrochem. Soc.* **1998**, 145, 2186.
- [35] K. Xhanari, M. Finšgar, *Arab J. Chem.* **2019**, 12, 4646.
- [36] P. R. Roberge, *Handbook of Corrosion Engineering*, The McGraw-Hill Companies, Inc., New York, NY **2000**.
- [37] L. Kobotiatis, N. Pebere, P. G. Koutsoukos, *Corros. Sci.* **1999**, 41, 941.
- [38] L. Garrigues, N. Pebere, F. Dabosi, *Electrochim. Acta* **1996**, 41, 1209.
- [39] E. E. Foad El-Sherbini, S. M. Abd-El-Wahab, M. A. Deyab, *Mater. Chem. Phys.* **2003**, 82, 631.
- [40] C. Edeleanu, U. R. Evans, *Trans. Faraday Soc.* **1951**, 47, 1121.
- [41] H. Kaesche, *Z. Für. Phys. Chem.* **1962**, 34, 87.
- [42] I. L. Müller, *Doctorate Thesis*, Universidad Nacional de Rosario, Comisión Nacional de Energía Atómica, Argentina, **1974**.
- [43] G. Bereket, A. Yurt, *Corros. Sci.* **2001**, 43, 1179.
- [44] B. Zaid, D. Saidi, A. Benzaid, S. Hadji, *Corros. Sci.* **2008**, 50, 1841.
- [45] M. Baumgärtner, H. Kaesche, *Mater. Corros.* **1991**, 42, 158.
- [46] I. L. Muller, J. R. Galvele, *Corros. Sci.* **1977**, 17, 179.
- [47] M. Pourbaix, *J. Common Met.* **1972**, 28, 51.
- [48] J. Zuo, M. Lei, R. Yang, Z. Liu, *J. Braz. Chem. Soc.* **2015**, 26, 410.
- [49] E. McCafferty, J. P. Wightman, *J. Colloid Interface Sci.* **1997**, 194, 344.
- [50] J. O. Bockris, L. V. Minevski, *J. Electroanal. Chem.* **1993**, 349, 375.
- [51] E. M. Sherif, S. M. Park, *J. Electrochem. Soc.* **2005**, 152, B205.
- [52] M. Baumgärtner, H. Kaesche, *Corros. Sci.* **1989**, 29, 363.
- [53] A. Y. Musa, A. A. H. Kadhum, A. B. Mohamad, M. S. Takriff, A. R. Daud, S. K. Kamarudin, *Corros. Sci.* **2010**, 52, 526.
- [54] F. S. de Souza, A. Spinelli, *Corros. Sci.* **2009**, 51, 642.
- [55] A. A. Hermas, M. S. Morad, *Corros. Sci.* **2008**, 50, 2710.
- [56] B. A. Shaw, G. D. Davis, T. L. Fritz, B. J. Rees, W. C. Mosher, *J. Electrochem. Soc.* **1991**, 138, 3288.
- [57] Z. Szklarska-Smialowska, *Corros. Sci.* **1999**, 41, 1743.
- [58] H. Ezuber, A. El-Houd, F. El-Shawesh, *Mater. Des.* **2008**, 29, 801.

- [59] G. S. Peng, K. H. Chen, H. C. Fang, H. Chao, S. Y. Chen, *Mater. Corros.* **2010**, *61*, 783.
- [60] V. H. Álvarez, S. Mattedi, M. Martin-Pastor, M. Aznar, M. Iglesias, *Fluid Phase Equilib.* **2010**, *299*, 42.
- [61] K. Sabet Bokati, C. Dehghanian, *J. Environ. Chem. Eng.* **2018**, *6*, 1613.
- [62] Q. Meng, G. S. Frankel, *J. Electrochem. Soc.* **2004**, *151*, B271.
- [63] I. L. Muller, J. R. Galvele, *Corros. Sci.* **1977**, *17*, 995.
- [64] K. Kowal, J. DeLuccia, J. Y. Josefowicz, C. Laird, G. C. Farrington, *J. Electrochem. Soc.* **1996**, *143*, 2471.
- [65] C. M. Liao, J. M. Olive, M. Gao, R. P. Wei, *Corrosion* **1998**, *54*, 451.
- [66] E. Barsoukov, J. R. Macdonald, *Impedance Spectroscopy, Theory Experiment and Applications*, 2nd ed., John Wiley & Sons, Inc, Hoboken, NJ **2005**.
- [67] M. N. El-Haddad, A. S. Fouda, *Chem. Eng. Commun.* **2013**, *200*, 1366.
- [68] N. Nnaji, N. Nwaji, J. Mack, T. Nyokong, *Molecules* **2019**, *24*, 207.
- [69] R. H. B. Beda, P. M. Niamien, E. B. Avo Bilé, A. Trokourey, *Adv. Chem.* **2017**, 6975248.

## SUPPORTING INFORMATION

Additional supporting information may be found online in the Supporting Information section.

**How to cite this article:** Ortega Vega RO, Mattedi S, Schroeder RM, Malfatti CdF. 2-hydroxyethylammonium oleate protic ionic liquid as corrosion inhibitor for aluminum in neutral medium. *Materials and Corrosion*. 2021;72: 543–556. <https://doi.org/10.1002/maco.202011847>